Eur. Phys. J. C (2019) 79:780
https://doi.org/10.1140/epjc/s10052-019-7302-6

THE EUROPEAN PHYSICAL JOURNAL C

Regular Article - Theoretical Physics

One-dimensional soliton system of gauged kink and Q-ball

A. Yu. Loginov[1,a], **V. V. Gauzshtein**[2,b]

[1] Tomsk State University of Control Systems and Radioelectronics, 634050 Tomsk, Russia
[2] Tomsk Polytechnic University, 634050 Tomsk, Russia

Received: 7 June 2019 / Accepted: 14 September 2019 / Published online: 20 September 2019

Abstract In the present paper, we consider a $(1 + 1)$-dimensional gauge model consisting of two complex scalar fields interacting with each other through an Abelian gauge field. When the model's gauge coupling constants are set to zero, the model possesses non-gauged Q-ball and kink solutions that do not interact with each other. It is shown here that for nonzero gauge coupling constants, the model has a soliton solution describing the system that consists of interacting Q-ball and kink components. These two components of the kink-Q-ball system have opposite electric charges, meaning that the total electric charge of the system vanishes. The properties of the kink-Q-ball system are studied both analytically and numerically. In particular, it was found that the system possesses a nonzero electric field and is unstable with respect to small perturbations in the fields.

1 Introduction

It is known that in the case of Maxwell electrodynamics, any one-dimensional or two-dimensional field configuration with a nonzero electric charge possesses infinite energy. The reason for this is simple: at large distances, the electric field of this configuration does not depend on the coordinate in the one-dimensional case, and behaves as r^{-1} in the two-dimensional case, meaning that the energy of the electric field diverges linearly in the one-dimensional case and logarithmically in the two-dimensional case. Hence, there are no electrically charged solitons in one and two dimensions; such solitons appear only in three dimensions (e.g. the three-dimensional electrically charged dyon [1] or Q-ball [2–5]). It should be noted, however, that electrically charged two-dimensional vortices exist in both the Chern–Simons [6–10] and the Maxwell–Chern–Simons [11–14] gauge models. Furthermore, it was shown in [15,16] that Chern–Simons gauge models also possess one-dimensional domain walls. The domain walls have finite linear densities of magnetic flux and electric charge, and thus there is a linear momentum flow along the domain walls.

However, even in the case of Maxwell gauge field models, there are electrically neutral low-dimensional soliton systems with a nonzero electric field in their interior areas. In particular, a one-dimensional soliton system consisting of electrically charged Q-ball and anti-Q-ball components was considered in [17], and a two-dimensional soliton system consisting of vortex and Q-ball components interacting through an Abelian gauge field was described in [18].

In the present paper, we examine a one-dimensional soliton system consisting of Q-ball and kink components with opposite electric charges, meaning that the system, which has a nonzero electric field, is electrically neutral as a whole. The properties of this kink-Q-ball system are investigated using both analytical and numerical methods. In particular, we find that unlike the non-gauged one-dimensional Q-ball, the kink-Q-ball system does not enter the thin-wall regime.

An interesting problem arises concerning the stability of the kink-Q-ball system with respect to small perturbations in the fields. Recall that the Abelian Higgs model possesses an electrically neutral kink solution [19,20]. Formally, this gauged kink solution is the usual kink of a self-interacting real scalar field up to gauge transformations. The properties of these two kink solutions differ considerably, since the classical vacua of the corresponding field models have a different topology. While the real kink is topologically stable, the gauged kink has a single unstable mode. From a topological point of view, the gauged kink lies between two topologically distinct vacua of the Abelian Higgs model, and thus is a sphaleron [19,20]. Note, however, that the gauged kink is a static field configuration modulo gauge transformation, whereas the kink-Q-ball system will depend on time in any gauge. Due to this fact, the kink-Q-ball system cannot be a sphaleron, and its classical stability therefore requires separate consideration.

[a] e-mail: aloginov@tpu.ru
[b] e-mail: gauzshtein@tpu.ru

This paper has the following structure. In Sect. 2, we describe briefly the Lagrangian, the symmetries, the field equations, and the energy-momentum tensor of the Abelian gauge model under consideration. In Sect. 3, we investigate the properties of the kink-Q-ball system. Using the Hamiltonian formalism and the Lagrange multipliers method, we establish the time dependence of the soliton system's fields. An important differential relation for the kink-Q-ball solution is derived and a system of nonlinear differential equations for ansatz functions is obtained. We then establish some general properties of the kink-Q-ball system. In particular, we examine the asymptotic behaviour of the system's fields at small and large distances, establish some important properties of the electromagnetic potential, and derive the virial relation for the soliton system. In Sect. 4, we study the properties of the kink-Q-ball system in three extreme regimes, i.e. in the thick-wall regime and the regimes of small and large gauge coupling constants. We also establish the basic properties of the plane-wave field configuration of the model. In Sect. 5, we present and discuss the numerical results obtained. They include the dependences of the energy of the kink-Q-ball system on its phase frequency and Noether charge, along with numerical results for the ansatz functions, the energy density, the electric charge density, and the electric field strength. We also present results for the classical stability of the kink-Q-ball system.

Throughout the paper, we use the natural units $\hbar = c = 1$.

2 The gauge model

The Lagrangian density of the $(1 + 1)$-dimensional gauge model under consideration has the form

$$\mathcal{L} = -\frac{1}{4}F_{\mu\nu}F^{\mu\nu} + (D_\mu\phi)^* D^\mu\phi - V(|\phi|) + (D_\mu\chi)^* D^\mu\chi - U(|\chi|), \tag{1}$$

where $F_{\mu\nu} = \partial_\mu A_\nu - \partial_\nu A_\mu$ is the strength of the Abelian gauge field and ϕ, χ are complex scalar fields that minimally interact with the Abelian gauge field through the covariant derivatives:

$$D_\mu\phi = \partial_\mu\phi + ieA_\mu\phi, \quad D_\mu\chi = \partial_\mu\chi + iqA_\mu\chi. \tag{2}$$

The self-interaction potentials of the scalar fields have the form

$$V(|\phi|) = \frac{\lambda}{2}(|\phi|^2 - \eta^2)^2, \tag{3}$$

$$U(|\chi|) = m_\chi^2 |\chi|^2 - \frac{g_\chi}{2}|\chi|^4 + \frac{h_\chi}{3}|\chi|^6. \tag{4}$$

Let us suppose that the self-interaction potential $U(|\chi|)$ has a global zero minimum at $\chi = 0$ and admits the existence of the usual non-gauged Q-balls. Then the parameters g_χ and h_χ are positive and satisfy the condition $3g_\chi^2 < 16h_\chi m_\chi^2$. Unlike the sixth-order potential $U(|\chi|)$, the fourth-order potential $V(|\phi|)$ reaches a zero minimum on the circle $|\phi| = \eta$. The potential $V(|\phi|)$ allows the existence of the complex non-gauged kink solution

$$\phi_{\mathrm{k}}(x) = \eta \tanh\left(\frac{m_\phi x}{2}\right)\exp(-i\delta), \tag{5}$$

where $m_\phi = \sqrt{2\lambda}\eta$ is the mass of the scalar ϕ-particle and δ is an arbitrary phase.

In addition to the local gauge transformations:

$$\phi(x) \to \phi'(x) = \exp(-ie\Lambda(x))\phi(x), \tag{6a}$$

$$\chi(x) \to \chi'(x) = \exp(-iq\Lambda(x))\chi(x), \tag{6b}$$

$$A_\mu(x) \to A'_\mu(x) = A_\mu(x) + \partial_\mu\Lambda(x), \tag{6c}$$

the Lagrangian (1) is also invariant under the two independent global gauge transformations:

$$\phi(x) \to \phi'(x) = \exp(-i\alpha)\phi(x), \tag{7a}$$

$$\chi(x) \to \chi'(x) = \exp(-i\beta)\chi(x). \tag{7b}$$

As a consequence, we have the two Noether currents:

$$j_\phi^\mu = i\left(\phi^* D^\mu\phi - \left(D^\mu\phi\right)^*\phi\right), \tag{8a}$$

$$j_\chi^\mu = i\left(\chi^* D^\mu\chi - \left(D^\mu\chi\right)^*\chi\right), \tag{8b}$$

and the two separately conserved Noether charges: $Q_\phi = \int_{-\infty}^{+\infty} j_\phi^0 dx$ and $Q_\chi = \int_{-\infty}^{+\infty} j_\chi^0 dx$. Note also that in addition to the local and global gauge transformations, the Lagrangian (1) is invariant under the discrete C, P, and T transformations.

The field equations of the model are written as

$$\partial_\mu F^{\mu\nu} = j^\nu, \tag{9}$$

$$D_\mu D^\mu\phi + \frac{\partial V}{\partial|\phi|}\frac{\phi}{2|\phi|} = 0, \tag{10}$$

$$D_\mu D^\mu\chi + \frac{\partial U}{\partial|\chi|}\frac{\chi}{2|\chi|} = 0, \tag{11}$$

where the electromagnetic current j^ν is written in terms of two Noether currents (8)

$$j^\nu = ej_\phi^\nu + qj_\chi^\nu. \tag{12}$$

From Eq. (12), it follows that the electric charges eQ_ϕ and qQ_χ of the complex scalar fields ϕ and χ are conserved separately. This is a consequence of the neutrality of the Abelian gauge field A_μ.

The symmetric energy-momentum tensor of the model can be obtained using the well-known formula $T_{\mu\nu} = 2\partial\mathcal{L}/\partial g^{\mu\nu} - g_{\mu\nu}\mathcal{L}$:

$$T_{\mu\nu} = -F_{\mu\lambda}F_{\nu}^{\ \lambda} + \frac{1}{4}g_{\mu\nu}F_{\lambda\rho}F^{\lambda\rho} + (D_\mu\phi)^* D_\nu\phi + (D_\nu\phi)^* D_\mu\phi + (D_\mu\chi)^* D_\nu\chi + (D_\nu\chi)^* D_\mu\chi - g_{\mu\nu}[(D_\mu\phi)^* D^\mu\phi + (D_\mu\chi)^* D^\mu\chi - V(|\phi|) - U(|\chi|)]. \quad (13)$$

Thus, we have the following expression for the energy density of the model

$$T_{00} = \mathcal{E} = \frac{1}{2}E_x^2 + (D_t\phi)^* D_t\phi + (D_x\phi)^* D_x\phi + (D_t\chi)^* D_t\chi + (D_x\chi)^* D_x\chi + V(|\phi|) + U(|\chi|), \quad (14)$$

where $E_x = F_{01} = \partial_t A_1 - \partial_x A_0$ is the electric field strength.

3 The kink-Q-ball system and its properties

It is known [21–23] that any nontopological soliton, and in particular a Q-ball, is an extremum of an energy functional at a fixed value of the corresponding Noether charge. Using this basic property of a Q-ball and taking into account the fact that the self-interaction potential $U(|\chi|)$ admits the existence of Q-balls formed from the complex scalar field χ, we search for a soliton solution to model (1) that is an extremum of the energy functional $E = \int_{-\infty}^{+\infty}\mathcal{E}dx$ at a fixed value of the Noether charge $Q_\chi = \int_{-\infty}^{+\infty} j_\chi^0 dx$. According to the method of Lagrange multipliers, such a solution is an unconditional extremum of the functional

$$F = \int_{-\infty}^{\infty}\mathcal{E}dx - \omega\int_{-\infty}^{\infty} j_\chi^0 dx = E - \omega Q_\chi, \quad (15)$$

where ω is the Lagrange multiplier. To determine the time dependence of the soliton solution, we use Eq. (15) and the Hamiltonian formalism. In the axial gauge $A_x = A^1 = 0$, the Hamiltonian density of model (1) is written as

$$\mathcal{H} = \pi_\phi\partial_t\phi + \pi_{\phi^*}\partial_t\phi^* + \pi_\chi\partial_t\chi + \pi_{\chi^*}\partial_t\chi^* - \mathcal{L} = -\frac{1}{2}(\partial_x A_0)^2 + \pi_\phi\pi_{\phi^*} + \pi_\chi\pi_{\chi^*} + \partial_x\phi^*\partial_x\phi + \partial_x\chi^*\partial_x\chi + ieA_0\left\{\phi^*\pi_{\phi^*} - \phi\pi_\phi\right\} + iqA_0\left\{\chi^*\pi_{\chi^*} - \chi\pi_\chi\right\} + V(|\phi|) + U(|\chi|). \quad (16)$$

We can see that in the adopted gauge, the model is described in terms of eight canonically conjugated fields: ϕ, $\pi_\phi = (D_0\phi)^*$, ϕ^*, $\pi_{\phi^*} = D_0\phi$, χ, $\pi_\chi = (D_0\chi)^*$, χ^*, and $\pi_{\chi^*} = D_0\chi$, while the time component A_0 of the gauge field is determined in terms of the canonically conjugated fields by Gauss's law

$$\partial_x^2 A_0 + ie\left\{\phi^*\pi_{\phi^*} - \phi\pi_\phi\right\} + iq\left\{\chi^*\pi_{\chi^*} - \chi\pi_\chi\right\} = 0, \quad (17)$$

and thus is not an independent dynamic field. Although energy density (14) is not equal to Hamiltonian density (16):

$$\mathcal{H} - \mathcal{E} = -(\partial_x A_0)^2 + ieA_0\left\{\phi^*\pi_{\phi^*} - \phi\pi_\phi\right\} + iqA_0\left\{\chi^*\pi_{\chi^*} - \chi\pi_\chi\right\}, \quad (18)$$

the integral of Eq. (18) over the one-dimensional space vanishes, provided that field configurations of the model possess finite energy and satisfy Gauss's law (17).

In the adopted axial gauge $A_x = 0$, field equations (10) and (11) can be recast in the Hamiltonian form:

$$\partial_t\phi = \frac{\delta H}{\delta\pi_\phi} = \frac{\delta E}{\delta\pi_\phi}, \quad \partial_t\pi_\phi = -\frac{\delta H}{\delta\phi} = -\frac{\delta E}{\delta\phi}, \quad (19)$$

$$\partial_t\chi = \frac{\delta H}{\delta\pi_\chi} = \frac{\delta E}{\delta\pi_\chi}, \quad \partial_t\pi_\chi = -\frac{\delta H}{\delta\chi} = -\frac{\delta E}{\delta\chi}, \quad (20)$$

where we use the relation $E = \int_{-\infty}^{+\infty}\mathcal{E}dx = H = \int_{-\infty}^{+\infty}\mathcal{H}dx$. On the other hand, the first variation of functional (15) vanishes on the soliton solution:

$$\delta F = \delta E - \omega\delta Q_\chi = 0, \quad (21)$$

where the first variation of the Noether charge Q_χ is expressed in terms of the canonically conjugated fields as follows:

$$\delta Q_\chi = -i\int_{-\infty}^{\infty}\left(\pi_\chi\delta\chi + \chi\delta\pi_\chi - \text{c.c.}\right)dx. \quad (22)$$

Combining Eqs. (19)–(22), we find that in the adopted gauge, only the time derivatives of the canonically conjugated fields χ, π_χ, χ^*, and π_{χ^*} are different from zero:

$$\partial_t\chi = \frac{\delta H}{\delta\pi_\chi} = \omega\frac{\delta Q_\chi}{\delta\pi_\chi} = -i\omega\chi, \quad (23)$$

$$\partial_t\pi_\chi = -\frac{\delta H}{\delta\chi} = -\omega\frac{\delta Q_\chi}{\delta\chi} = i\omega\pi_\chi, \quad (24)$$

$$\partial_t\chi^* = \frac{\delta H}{\delta\pi_{\chi^*}} = \omega\frac{\delta Q_\chi}{\delta\pi_{\chi^*}} = i\omega\chi^*, \quad (25)$$

$$\partial_t\pi_{\chi^*} = -\frac{\delta H}{\delta\chi^*} = -\omega\frac{\delta Q_\chi}{\delta\chi^*} = -i\omega\pi_{\chi^*}, \quad (26)$$

while the time derivatives of ϕ, π_ϕ, ϕ^*, and π_{ϕ^*} are equal to zero. Recalling that $\pi_\chi = (D_0\chi)^* = \partial_t\chi^* - iqA_0\chi^*$ and taking into account Eqs. (24) and (25), we conclude that the time derivative of A_0 also vanishes. It follows that only the scalar field χ of the soliton system has nontrivial time dependence:

$$\phi(x,t) = f(x), \quad (27a)$$

$$\chi(x,t) = s(x)\exp(-i\omega t), \quad (27b)$$

$$A_\mu(x,t) = (a_0(x), 0). \tag{27c}$$

We now return to Eq. (21). This equation holds for arbitrary variations of fields on the soliton solution, including those that change the soliton solution to an infinitesimally close one. It follows that the energy of the soliton system satisfies the important relation

$$\frac{dE}{dQ_\chi} = \omega, \tag{28}$$

where the Lagrange multiplier ω is some function of the Noether charge Q_χ. Since the energy E and the Noether charge Q_χ of the soliton system are gauge-invariant, relation (28) is also gauge-invariant. In a similar way to the case of non-gauged nontopological solitons [21–23], relation (28) determines the basic properties of the gauged kink-Q-ball system.

In Eq. (27), the functions $f(x)$ and $s(x)$ are assumed to be complex functions of the real argument x. Substituting Eq. (27) into field equations (9)–(11), we can easily check that the real and imaginary parts of $f(x)$ satisfy the same differential equation with real coefficients. Similarly, the real and imaginary parts of $s(x)$ also satisfy the same differential equation with real coefficients. It follows that the functions $f(x)$ and $s(x)$ have the forms $f(x) = \exp(i\alpha)\tilde{f}(x)$, $s(x) = \exp(i\beta)\tilde{s}(x)$, where $\tilde{f}(x)$ and $\tilde{s}(x)$ are real functions, whereas α and β are constant phases. However, these phases can be cancelled by global gauge transformations (7), and the functions $f(x)$ and $s(x)$ can therefore be assumed to be real without loss of generality. The functions $a_0(x)$, $f(x)$, and $s(x)$ satisfy the system of ordinary nonlinear differential equations:

$$a_0''(x) - 2a_0(x)(e^2 f(x)^2 + q^2 s(x)^2) + 2q\omega s(x)^2 = 0, \tag{29}$$

$$f''(x) + (\lambda\eta^2 + e^2 a_0(x)^2) f(x) - \lambda f(x)^3 = 0, \tag{30}$$

$$s''(x) - (m_\chi^2 - (\omega - q a_0(x))^2) s(x) + g_\chi s(x)^3 - h_\chi s(x)^5 = 0, \tag{31}$$

which is obtained by substituting Eq. (27) into field equations (9)–(11).

The most important local quantities of the kink-Q-ball system are the electromagnetic current density and the energy density. They can be expressed in terms of $a_0(x)$, $f(x)$, and $s(x)$ as

$$j^\mu = (2q\omega s^2 - 2a_0(e^2 f^2 + q^2 s^2),\ 0), \tag{32}$$

$$\mathcal{E} = \frac{a_0'^2}{2} + f'^2 + s'^2 + (\omega - q a_0)^2 s^2 + e^2 a_0^2 f^2 + V(f) + U(s). \tag{33}$$

The energy $E = \int_{-\infty}^{+\infty} \mathcal{E} dx$ of the kink-Q-ball system must be finite. Using this fact and Eq. (33), we obtain the boundary conditions for $a_0(x)$, $f(x)$, and $s(x)$:

$$a_0(x) \underset{x\to-\infty}{\longrightarrow} 0, \quad a_0(x) \underset{x\to\infty}{\longrightarrow} 0, \tag{34a}$$

$$f(x) \underset{x\to-\infty}{\longrightarrow} -\eta, \quad f(x) \underset{x\to\infty}{\longrightarrow} \eta, \tag{34b}$$

$$s(x) \underset{x\to-\infty}{\longrightarrow} 0, \quad s(x) \underset{x\to\infty}{\longrightarrow} 0. \tag{34c}$$

Note that the finiteness of the electric field energy $E^{(E)} = \int_{-\infty}^{+\infty} a_0'^2/2 dx$ leads to further boundary conditions for $a_0(x)$:

$$a_0'(x) \underset{x\to-\infty}{\longrightarrow} 0, \quad a_0'(x) \underset{x\to\infty}{\longrightarrow} 0. \tag{35}$$

These conditions, however, follow from Eq. (34a), provided that $a_0(x)$ is regular as $x \to \pm\infty$.

Gauss's law (29) can be written as $a_0'' = -j^0$, where j^0 is electric charge density (32). Integrating this equation over $x \in (-\infty, \infty)$ and taking into account boundary conditions (35), we conclude that the total electric charge $Q = \int_{-\infty}^{+\infty} j^0 dx$ of a field configuration with finite energy vanishes:

$$Q = eQ_\phi + qQ_\chi = 0, \tag{36}$$

where Q_ϕ and Q_χ are the Noether charges defined in Eq. (8).

It can easily be checked that system (29)–(31) is invariant under the discrete transformation

$$\omega, a_0, f, s \longrightarrow -\omega, -a_0, f, s. \tag{37}$$

This invariance is a consequence of the C-invariance of the Lagrangian (1). Using Eqs. (32), (33), and (37), we can find the behaviour of the energy E and the Noether charges Q_ϕ and Q_χ under the transformation $\omega \to -\omega$:

$$E(-\omega) = E(\omega), \tag{38}$$

$$Q_{\phi,\chi}(-\omega) = -Q_{\phi,\chi}(\omega). \tag{39}$$

We see that the energy of the kink-Q-ball system is an even function of ω, whereas the Noether charges Q_ϕ and Q_χ are odd functions of ω.

The P-invariance of the Lagrangian (1) leads to the invariance of system (29)–(31) under the space inversion $x \to -x$. Due to the space homogeneity, system (29)–(31) is also invariant under the coordinate shift $x \to x + x_0$. Furthermore, due to Eqs. (7), system (29)–(31) is invariant under the two independent discrete transformations: $f \to -f$ and $s \to -s$. These facts and the symmetry properties of boundary conditions (34) lead to the conclusion that $a_0(x)$ and $s(x)$ are even functions of x, while $f(x)$ is an odd function of x. This is consistent with the fact that the non-gauged kink solution is an odd function of x, whereas the non-gauged Q-ball solution is an even function of x.

The asymptotic form of the soliton solution for small x is obtained by substitution of the power expansions for $a_0(x)$, $f(x)$, and $s(x)$ into Eqs. (29)–(31) and equating the resulting Taylor coefficients to zero. In this way, we obtain:

$$a_0(x) = a_0 + \frac{a_2}{2!}x^2 + O(x^3), \tag{40a}$$

$$f_0(x) = f_1 x + \frac{f_3}{3!}x^3 + O(x^5), \tag{40b}$$

$$s_0(x) = s_0 + \frac{s_2}{2!}x^2 + O(x^3), \tag{40c}$$

where the coefficients in the second terms

$$a_2 = -2qs_0^2(\omega - qa_0), \tag{41a}$$

$$f_3 = -\frac{1}{2}f_1(m_\phi^2 + 2e^2a_0^2), \tag{41b}$$

$$s_2 = s_0(m_\chi^2 - (\omega - qa_0)^2) - g_\chi s_0^3 + h_\chi s_0^5 \tag{41c}$$

are expressed in terms of the three leading coefficients a_0, f_1, s_0, and the parameters of the model.

For large $|x|$, system (29)–(31) is linearized, and we obtain an asymptotic form of the soliton solution satisfying boundary conditions (34):

$$f(x) \sim \pm\eta \pm f_\infty \exp\left(\mp m_\phi x\right), \tag{42a}$$

$$s(x) \sim s_\infty \exp\left(\mp \Delta x\right), \tag{42b}$$

$$a_0(x) \sim a_\infty \exp\left(\mp m_A x\right) - \frac{2q\omega}{4\Delta^2 - m_A^2}s_\infty^2 \exp\left(\mp 2\Delta x\right), \tag{42c}$$

where $m_\phi = \sqrt{2\lambda}\eta$, $\Delta = (m_\chi^2 - \omega^2)^{1/2}$, and $m_A = \sqrt{2}e\eta$.

We now turn to the global behaviour of the electromagnetic potential $a_0(x)$. Since the total electric charge $Q = \int_{-\infty}^{+\infty} j^0(x)\,dx$ of the kink-Q-ball system vanishes, the electric charge density $j^0(x)$ must vanish at some points of the x-axis. Due to the symmetry $j^0(-x) = j^0(x)$, these points (nodes of $j^0(x)$) are symmetric with respect to the origin $x = 0$. Next, according to Gauss's law $a_0''(x) = -j^0(x)$, the second derivative $a_0''(x)$ vanishes at the nodes of $j^0(x)$. Thus, the nodes of $j^0(x)$ are the inflection points of the electromagnetic potential $a_0(x)$. From Eq. (29) it follows that at an inflection point x_i, the electromagnetic potential $a_0(x_\mathrm{i})$ can be expressed in terms of $f(x_\mathrm{i})$ and $s(x_\mathrm{i})$:

$$a_0(x_\mathrm{i}) = \frac{\omega q s(x_\mathrm{i})^2}{e^2 f(x_\mathrm{i})^2 + q^2 s(x_\mathrm{i})^2}. \tag{43}$$

Two conclusions follow from Eq. (43). Firstly, at an inflection point x_i, the sign of $a_0(x_\mathrm{i})$ coincides with the sign of ω (we assume that the gauge coupling constants are positive):

$$\mathrm{sign}\left(a_0(x_\mathrm{i})\right) = \mathrm{sign}(\omega). \tag{44}$$

Secondly, at an inflection point x_i, the following inequality holds:

$$|a_0(x_\mathrm{i})| < \frac{|\omega|}{q}. \tag{45}$$

Next, from Eq. (32), we obtain the expression for the electric charge density at the origin:

$$j^0(0) = -a_0''(0) = 2qs(0)^2(\omega - qa_0(0)), \tag{46}$$

from which it follows that the sign of the curvature of $a_0(x)$ at $x = 0$ is opposite in sign to $\omega - qa_0(0)$:

$$\mathrm{sign}\left(a_0''(0)\right) = -\mathrm{sign}(\omega - qa_0(0)). \tag{47}$$

An elementary graphical analysis carried out using Eqs. (43)–(47) leads us to the following conclusions about the behaviour of $a_0(x)$:

$$0 < a_0(\pm x_{\mathrm{i}1}) < a_0(0) < \frac{\omega}{q} \quad \text{for} \quad \omega > 0, \tag{48}$$

and

$$\frac{\omega}{q} < a_0(0) < a_0(\pm x_{\mathrm{i}1}) < 0 \quad \text{for} \quad \omega < 0, \tag{49}$$

where $\pm x_{\mathrm{i}1}$ represents the two symmetric inflection points closest to the origin, $x = 0$. From Eqs. (46), (48), and (49), it follows that the sign of the electric charge density at the origin coincides with that of the phase frequency

$$\mathrm{sign}\left(j^0(0)\right) = -\mathrm{sign}\left(a_0''(0)\right) = \mathrm{sign}(\omega). \tag{50}$$

We can also draw conclusions about the behaviour of $a_0(x)$ for $|x| > x_{\mathrm{i}1}$. In particular, $a_0(x)$ cannot vanish at any finite x. If we let x_n be a conjectural point in which $a_0(x)$ vanishes, then from Eq. (29) we have the relation

$$a_0''(x_\mathrm{n}) = -2q\omega s(x_\mathrm{n})^2. \tag{51}$$

We see that the sign of the curvature of $a_0(x)$ at the point x_n is opposite to the sign of ω. If we assume ω is positive, then it follows from Eq. (51) that in some neighbourhood of x_n, the functions $a_0(x)$ and $a_0''(x)$ are negative; however according to Eq. (44), there are no inflection points for negative $a_0(x)$, meaning that $a_0''(x)$ can never change sign, $a_0(x)$ decreases indefinitely, and boundary condition (34a) cannot be satisfied. It follows that $a_0(x)$ cannot vanish at any finite x. The case of negative ω is treated similarly. Thus, we come to the important conclusion that the electromagnetic potential $a_0(x)$ cannot vanish at any finite x, and so the sign of

the electromagnetic potential coincides with that of the phase frequency over the whole range of x:

$$\text{sign}\,(a_0\,(x)) = \text{sign}\,(\omega) \tag{52}$$

for all x. Of course, this conclusion is valid only for adopted gauge (27c).

Let $a_0\,(x)$, $f\,(x)$, and $s\,(x)$ be a solution of system (29)–(31) that satisfies boundary conditions (34). When we perform the scale transformation $x \to \lambda x$ of the argument of the solution, the Lagrangian $L = \int_{-\infty}^{+\infty} \mathcal{L} dx$ becomes a simple function of the scale parameter λ. The function $L\,(\lambda)$ must have an extremum at $\lambda = 1$, and so the derivative $dL/d\lambda$ vanishes at this point. Using this fact, we obtain the virial relation for the soliton system:

$$E^{(E)} + E^{(P)} - E^{(G)} - E^{(T)} = 0, \tag{53}$$

where

$$E^{(E)} = \int\limits_{-\infty}^{\infty} \frac{a_0'^2}{2} dx \tag{54}$$

is the electric field energy;

$$E^{(G)} = \int\limits_{-\infty}^{\infty} (f'^2 + s'^2) dx \tag{55}$$

is the gradient part of the soliton's energy;

$$E^{(T)} = \int\limits_{-\infty}^{\infty} \left((\omega - q a_0)^2 s^2 + e^2 a_0^2 f^2\right) dx \tag{56}$$

is the kinetic part of the soliton's energy; and

$$E^{(P)} = \int\limits_{-\infty}^{\infty} (V\,(f) + U\,(s))\, dx \tag{57}$$

is the potential part of the soliton's energy.

The energy E of the soliton system is the sum of terms (54)–(57). Using this fact and virial relation (54), we obtain two representations for the energy of the soliton system:

$$E = 2(E^{(T)} + E^{(G)}) = 2(E^{(P)} + E^{(E)}). \tag{58}$$

Another representation for the energy of the soliton system can be obtained by integrating the term $a_0'^2/2$ in Eq. (33) by parts, and using Eqs. (29), (32), and (34):

$$E = \frac{1}{2}\omega Q_\chi + E^{(G)} + E^{(P)}. \tag{59}$$

Finally, using Eq. (59), we obtain the relation between the Noether charge Q_χ, the electric field energy $E^{(E)}$, and the kinetic energy $E^{(T)}$:

$$\omega Q_\chi = 2(E^{(E)} + E^{(T)}). \tag{60}$$

Let us show that if we know a particular soliton solution of model (1), we also know a one-parameter family of rescaled soliton solutions. Following [23], we form the two dimensionless combinations:

$$\epsilon = \left[16 h_\chi m_\chi^2 / \left(3 g_\chi^2\right) - 1\right]^{1/2},$$
$$g = 2\left[h_\chi / \left(3 g_\chi\right)\right]^{1/2}. \tag{61}$$

Since the condition $3g_\chi^2 < 16 h_\chi m_\chi^2$ is assumed to be fulfilled, the parameter ϵ is real. The coupling constants g_χ and h_χ are expressed in terms of g and ϵ as follows:

$$g_\chi = g^2 \bar{g}_\chi,\ h_\chi = g^4 \bar{h}_\chi, \tag{62}$$

where the rescaled coupling constants $\bar{g}_\chi$ and $\bar{h}_\chi$ are

$$\bar{g}_\chi = \frac{4 m_\chi^2}{1+\epsilon^2} = \frac{3}{4}\frac{g_\chi^2}{h_\chi}, \tag{63}$$

$$\bar{h}_\chi = \frac{3 m_\chi^2}{1+\epsilon^2} = \frac{9}{16}\frac{g_\chi^2}{h_\chi}, \tag{64}$$

giving $\bar{h}_\chi = 3\bar{g}_\chi/4$. Next, we use the dimensionless parameter g to rescale the fields of the model and the remaining coupling constants as follows: $\phi = g^{-1}\bar{\phi}$, $\chi = g^{-1}\bar{\chi}$, $\eta = g^{-1}\bar{\eta}$, $A^\mu = g^{-1}\bar{A}^\mu$, $\lambda = g^2\bar{\lambda}$, $e = g\bar{e}$, and $q = g\bar{q}$. Note that the mass $m_\phi = \sqrt{2\lambda}\eta$ of the Higgs field ϕ_H, the mass $m_A = \sqrt{2}e\eta$ of the gauge field A^μ, and the parameter ϵ are invariant under rescaling, whereas the mass m_χ of the complex scalar field χ is not subjected to rescaling.

In terms of the rescaled fields and coupling constants, self-interaction potentials (3) and (4) can be written as:

$$U\,(|\chi|) = \frac{1}{g^2}\frac{m_\chi^2}{1+\epsilon^2}|\bar{\chi}|^2\left[\left(1 - |\bar{\chi}|^2\right)^2 + \epsilon^2\right], \tag{65}$$

$$V\,(|\phi|) = \frac{1}{g^2}\frac{m_\phi^2\bar{\eta}^2}{4}\left(\frac{|\bar{\phi}|^2}{\bar{\eta}^2} - 1\right)^2, \tag{66}$$

and thus the dependence on the parameter g is factorized. Using Eqs. (65) and (66), it can be shown that the Lagrangian (1) has the following behaviour under rescaling:

$$\mathcal{L}\left(\phi, \chi, A^\mu, m_\phi, \eta, m_\chi, g, \epsilon, e, q\right) = g^{-2}\bar{\mathcal{L}}\left(\bar{\phi}, \bar{\chi}, \bar{A}^\mu, m_\phi, \bar{\eta}, m_\chi, \epsilon, \bar{e}, \bar{q}\right), \tag{67}$$

where rescaled Lagrangian $\bar{\mathcal{L}}\left(\bar{\phi}, \bar{\chi}, \bar{A}^\mu, m_\phi, \bar{\eta}, m_\chi, \epsilon, \bar{e}, \bar{q}\right)$ is $\mathcal{L}\left(\bar{\phi}, \bar{\chi}, \bar{A}^\mu, m_\phi, \bar{\eta}, m_\chi, 1, \epsilon, \bar{e}, \bar{q}\right)$, and thus does not

depend on the parameter g. Next, Eq. (67) can be written in the form

$$\begin{aligned}&\mathcal{L}\left(\kappa^{-1}\phi, \kappa^{-1}\chi, \kappa^{-1}A^{\mu}, m_{\phi}, \kappa^{-1}\eta, m_{\chi}, \kappa g, \epsilon, \kappa e, \kappa q\right)\\&\quad=(\kappa g)^{-2}\,\bar{\mathcal{L}}\left(\bar{\phi}, \bar{\chi}, \bar{A}^{\mu}, m_{\phi}, \bar{\eta}, m_{\chi}, \epsilon, \bar{e}, \bar{q}\right)\\&\quad=\kappa^{-2}\mathcal{L}\left(\phi, \chi, A^{\mu}, m_{\phi}, \eta, m_{\chi}, g, \epsilon, e, q\right),\end{aligned}\tag{68}$$

where κ is an arbitrary positive scale factor. From Eq. (68) it follows that field equations (9)–(11) are invariant under rescaling. Hence, if (ϕ, χ, A^{μ}) is a solution corresponding to the parameters m_{χ}, g_{χ}, h_{χ}, η, λ, e, and q, then $\left(\kappa^{-1}\phi, \kappa^{-1}\chi, \kappa^{-1}A^{\mu}\right)$ is also a solution corresponding to the parameters $m_{\chi}, \kappa^{2}g_{\chi}, \kappa^{4}h_{\chi}, \kappa^{-1}\eta, \kappa^{2}\lambda, \kappa e$, and κq.

Finally, the energy density and the Noether charge densities behave under rescaling as follows:

$$\mathcal{E}\left(\kappa^{-1}\phi, \kappa^{-1}\chi, \kappa^{-1}A^{\mu}\right)=\kappa^{-2}\mathcal{E}\left(\phi, \chi, A^{\mu}\right),\tag{69}$$

$$j^{0}_{\phi}\left(\kappa^{-1}\phi, \kappa^{-1}A^{\mu}, \kappa e\right)=\kappa^{-2}j^{0}_{\phi}\left(\phi, A^{\mu}, e\right),\tag{70}$$

$$j^{0}_{\chi}\left(\kappa^{-1}\chi, \kappa^{-1}A^{\mu}, \kappa q\right)=\kappa^{-2}j^{0}_{\chi}\left(\chi, A^{\mu}, q\right),\tag{71}$$

where we omit the lists of parameters in Eq. (69) (which are the same as in Eq. (68)) for brevity. From Eqs. (69)–(71) it follows that the energy and the Noether charges of the kink-Q-ball system increase with a decrease in the scale factor κ.

4 Extreme regimes of the kink-Q-ball system

In this section, we will first examine the properties of the kink-Q-ball system in the thick-wall regime [24–26]. In this regime, the parameter $\Delta=(m_{\chi}^{2}-\omega^{2})^{1/2}$ tends to zero, meaning that the absolute value of the phase frequency tends to m_{χ}. From Eq. (42), it follows that in the thick-wall regime, the functions $s(x)$ and $a_0(x)$ are spread over the one-dimensional space, whereas the asymptotic behaviour of $f(x)$ remains unchanged. In the thick-wall regime, the functions $s(x)$ and $a_0(x)$ uniformly decrease as Δ and Δ^2, respectively, while the function $f(x)$ tends to non-gauged kink solution (5). In view of this, we perform the following scale transformation of the fields and the x-coordinate:

$$x=\frac{\bar{x}}{\Delta},\ s(x)=\frac{\Delta}{m_{\chi}}\bar{s}(\bar{x}),\ a_0(x)=\frac{\Delta^{2}}{m_{\chi}^{2}}\bar{a}_0(\bar{x}),\tag{72}$$

while the field $f(x)$ is taken to be equal to that of kink solution (5). To investigate the properties of the kink-Q-ball system in the thick-wall regime, we use functional (15), which is related to the energy functional through the Legendre transformation $F(\omega)=E\left(Q_{\chi}\right)-\omega Q_{\chi}$. Using scale transformation (72), we can determine the leading term of the dependence of the functional $F(\omega)$ on ω in the thick-wall regime:

$$F(\omega)=E_{\mathrm{k}}+\Delta^{3}m_{\chi}^{-2}\bar{F}+O(\Delta^{5}),\tag{73}$$

where $E_k=4\eta^{3}\sqrt{2\lambda}/3=4\eta^{2}m_{\phi}/3$ is the rest energy of the non-gauged kink and the dimensionless functional $\bar{F}$ does not depend on ω:

$$\bar{F}=\int_{-\infty}^{\infty}\left[\bar{s}'(\bar{x})^{2}+\bar{s}(\bar{x})^{2}-\frac{g_{\chi}}{2m_{\chi}^{2}}\bar{s}(\bar{x})^{4}\right]d\bar{x}.\tag{74}$$

In Eq. (73), higher-order terms in Δ may be neglected in the thick-wall regime, and thus we can sequentially obtain:

$$Q_{\chi}(\omega)=-\frac{dF(\omega)}{d\omega}=3\bar{F}m_{\chi}^{-2}\omega\left(m_{\chi}^{2}-\omega^{2}\right)^{\frac{1}{2}},\tag{75}$$

$$\begin{aligned}E(\omega)&=F(\omega)-\omega\frac{dF(\omega)}{d\omega}\\&=E_{\mathrm{k}}+\bar{F}m_{\chi}^{-2}\left(2\omega^{2}+m_{\chi}^{2}\right)\left(m_{\chi}^{2}-\omega^{2}\right)^{\frac{1}{2}},\end{aligned}\tag{76}$$

where the known properties of the Legendre transformation are used. From Eqs. (75) and (76), we obtain the energy of the kink-Q-ball system as a function of its Noether charge in the thick-wall regime:

$$E=E_{\mathrm{k}}+m_{\chi}Q_{\chi}-\frac{1}{9\times 3!}\frac{m_{\chi}}{\bar{F}^{2}}Q_{\chi}^{3}+Q\left(Q_{\chi}^{5}\right).\tag{77}$$

Next, we consider two opposite extreme regimes. In the first regime, the gauge coupling constants e and q tend to zero, whereas in the second they tend to infinity. In both regimes, the ratio $\varrho=eq^{-1}$ of the gauge coupling constants is a constant value. Since system of differential equations (29)–(31) is invariant under the transformation $e\to -e$, we may suppose without loss of generality that ϱ is positive. Moreover, system (29)–(31) is also invariant under the transformation $e\to -e$, $q\to -q$, $a_0\to -a_0$, as are the soliton energy and the Noether charges. It follows that both gauge coupling constants may be considered as positive without loss of generality.

When the gauge coupling constants e and q vanish, the gauge field $A_{\mu}=(a_0(x),\ 0)$ is decoupled from the kink-Q-ball system, which thus becomes a set of non-gauged kink and Q-ball solutions that do not interact with each other. In this connection, we want to ascertain the behaviour of the gauge potential $a_0(x)$ as $e=\varrho q\to 0$. To do this, we use expressions (40a) and (42c) for $a_0(x)$, which are valid for small and large values of $|x|$, respectively. We also assume that Eqs. (40a) and (42c) qualitatively describe the behaviour of a_0 at intermediate $|x|$. Equations (40a) and (42c) depend on the free parameters a_0 and a_{∞}, respectively, which can be determined by the condition of continuity of $a_0(x)$ and $a_0'(x)$ at some intermediate x. As a result, a_0 and a_{∞} become functions of the parameters of the model, including the gauge coupling constants e and q. It can be shown that a_0 and a_{∞}

tend to the same nonzero limit as $e = \varrho q \to 0$. It follows that at any finite x, the gauge potential $a_0(x)$ tends asymptotically to a constant as $e = \varrho q \to 0$:

$$\lim_{e=\varrho q\to 0} a_0(x, e, q) = \alpha, \tag{78}$$

where the limiting value α depends on the model's parameters and ϱ.

Let us consider the behaviour of the gauge potential $a_0(x)$ at small values of e and q in more detail. If the gauge coupling constants e and q are arbitrarily small but different from zero, the gauge potential $a_0(x)$ satisfies boundary conditions (34a) and (35). The first boundary condition provides the finite contribution of the term $e^2 a_0(x)^2 f(x)^2$ to the soliton energy, while the second one does the same for the contribution of the electric field energy density $a_0'^2/2$. When the gauge coupling constants e and q tend to zero (i.e., e and q are arbitrarily small but nonzero), boundary conditions (34a) and (35) hold. In this case, according to Eq. (78), the gauge potential $a_0(x)$ tends asymptotically to the constant α at any finite x. That is, for any finite x and arbitrarily small positive ϵ, there exists the arbitrarily small positive $\delta(\epsilon, x)$ such that $|a_0(x) - \alpha| < \epsilon$ if $e = \varrho q < \delta$. Nevertheless, at arbitrarily small but nonzero e and q, the gauge potential $a_0(x)$ tends to zero as $x \to \pm\infty$. However, if $e = \varrho q = 0$, the term $e^2 a_0(x)^2 f(x)^2$ in Eq. (33) vanishes, meaning that boundary condition (34a) becomes unnecessary and only the less stringent boundary condition (35) holds. In this case, we have the nonzero constant solution $a_0(x) = \alpha$, where α is equal to limiting value (78) to which the electromagnetic potential $a_0(x)$ tends asymptotically as $e = \varrho q \to 0$. We conclude that the behaviour of the electromagnetic potential $a_0(x, e, q)$ is nonregular in neighbourhoods of the infinitely remote points with $(e, q, x) = (0, 0, \pm\infty)$. Indeed, it follows from the foregoing that in a close neighbourhood of $e = \varrho q = 0$, $\lim_{x\to\pm\infty} a_0\left(x, e, \varrho^{-1}e\right) = \alpha\delta_{0e}$, where δ_{0e} is the Kronecker delta.

Equation (78) and the linearization of Eqs. (30) and (31) lead us to the asymptotic forms of $f(x)$ and $s(x)$ at small gauge coupling constants:

$$f(x) = f_{\mathrm{k}}(x) + e^2 f_2(x) + O(e^4), \tag{79a}$$
$$s(x) = s_{\mathrm{q}}(x) + e s_1(x) + O(e^2), \tag{79b}$$

where $f_{\mathrm{k}}(x)$ and $s_{\mathrm{q}}(x)$ are the non-gauged kink and Q-ball solutions, respectively, and $f_2(x)$ and $s_1(x)$ are some regular functions that depend on the parameters of the model (except for e and q) and ϱ. Note that due to the relation $e = \varrho q$, we use only one expansion parameter e. Substituting Eqs. (78) and (79) into Eq. (32), we find the asymptotic behaviour of the Noether charges Q_ϕ and Q_χ as $e = \varrho q \to 0$:

$$Q_\chi = -\varrho Q_\phi = Q_0 + e Q_1 + O(e^2), \tag{80}$$

where $Q_0 = 2\omega \int_{-\infty}^{+\infty} s_{\mathrm{q}}^2 dx$ is the Noether charge of the non-gauged Q-ball and the coefficient Q_1 depends on the parameters of the model (except for e and q) and ϱ. Similarly to Eq. (80), we obtain the asymptotic behaviour of the components of the soliton energy (54)–(57) and the total soliton energy:

$$E^{(E)} = e E_1^{(E)} + O(e^2), \tag{81a}$$
$$E^{(G)} = E_0^{(G)} + e E_1^{(G)} + O(e^2), \tag{81b}$$
$$E^{(T)} = E_0^{(T)} + e E_1^{(T)} + O(e^2), \tag{81c}$$
$$E^{(P)} = E_0^{(P)} + e E_1^{(P)} + O(e^2), \tag{81d}$$
$$E = E_0 + e E_1 + O(e^2), \tag{81e}$$

where $E_0^{(G)} = \int_{-\infty}^{+\infty} (f_{\mathrm{k}}'^2 + s_{\mathrm{q}}'^2) dx$, $E_0^{(T)} = \omega^2 \int_{-\infty}^{+\infty} s_{\mathrm{q}}^2 dx$, and $E_0^{(P)} = \int_{-\infty}^{+\infty} \left(V(f_{\mathrm{k}}) + U\left(s_{\mathrm{q}}\right)\right) dx$ are the gradient, kinetic, and potential parts of the energy of the non-gauged soliton system, respectively; $E_0 = E_0^{(G)} + E_0^{(T)} + E_0^{(P)}$ is the total energy of the non-gauged soliton system; and the coefficients $E_1^{(E)}$, $E_1^{(G)}$, $E_1^{(T)}$, and $E_1^{(P)}$ depend on the parameters of the model (except for e and q) and ϱ. Note that the non-gauged solutions f_{k} and s_{q} can be expressed in analytical form, as can the corresponding energies and the Noether charges. The corresponding expressions for the one-dimensional non-gauged Q-ball are given in [17]. Thus the coefficients Q_0, $E_0^{(G)}$, $E_0^{(T)}$, $E_0^{(P)}$, and E_0 can also be expressed in analytical form.

We now turn to a study of the opposite regime in which both gauge coupling constants tend to infinity: $e = \varrho q \to \infty$. We assume that the behaviour of the electromagnetic potential $a_0(x)$ in a neighbourhood of $x = 0$ is regular, and thus the coefficient a_2 given in Eq. (41a) is either finite or tends to zero as $e = \varrho q \to \infty$. However, from Eqs. (29) and (31) it follows that the electromagnetic potential is an odd function of q: $a_0(x, -q) = -a_0(x, q)$. Thus, we conclude that $a_2 \propto q^{-1}$ in the leading order, and so from Eq. (41a) it follows that $a_0 = \omega q^{-1} + a_{-3} q^{-3} + O\left(q^{-5}\right)$, where a_{-3} is a constant. This suggests that the electromagnetic potential $a_0(x)$ has a similar asymptotic expansion

$$a_0(x) = e^{-1} a_{-1}(x) + e^{-3} a_{-3}(x) + O(e^{-5}), \tag{82}$$

where the relation $e = \varrho q$ is used. In Eq. (82), $a_{-1}(x)$ and $a_{-3}(x)$ are some regular functions that depend on the parameters of the model (except for e and q) and ϱ. Using Eqs. (30), (31), and (82), we obtain the asymptotic expansions for $f(x)$ and $s(x)$:

$$f(x) = f_0(x) + e^{-2} f_{-2}(x) + O(e^{-4}), \tag{83a}$$
$$s(x) = s_0(x) + e^{-2} s_{-2}(x) + O(e^{-4}), \tag{83b}$$

where $f_0(x)$, $f_{-2}(x)$, $s_0(x)$, and $s_{-2}(x)$ are regular functions depending on the parameters of the model (except for e and q) and ϱ. In a similar way to Eqs. (78) and (79), we can

use Eqs. (82) and (83) to obtain asymptotic expansions for the components of the soliton energy, the total energy, and the Noether charges:

$$E^{(E)} = e^{-2}E^{(E)}_{-2} + O(e^{-4}), \tag{84a}$$
$$E^{(G)} = \widetilde{E}^{(G)}_{0} + e^{-2}E^{(G)}_{-2} + O(e^{-4}), \tag{84b}$$
$$E^{(T)} = \widetilde{E}^{(T)}_{0} + e^{-2}E^{(T)}_{-2} + O(e^{-4}), \tag{84c}$$
$$E^{(P)} = \widetilde{E}^{(P)}_{0} + e^{-2}E^{(P)}_{-2} + O(e^{-4}), \tag{84d}$$
$$E = \widetilde{E}_{0} + e^{-2}E_{-2} + O(e^{-4}), \tag{84e}$$
$$Q_{\chi} = -\varrho Q_{\phi} = \widetilde{Q}_{0} + e^{-2}Q_{-2} + O(e^{-4}), \tag{84f}$$

where we use the tilde to distinguish the corresponding coefficients from those of Eqs. (80) and (81). We see that as $e = \varrho q \to \infty$, the gauge field $a_0(x)$ tends to zero, meaning that the electric field's energy $E^{(E)}$ also vanishes in this regime. At the same time, the products $ea_0(x)$ and $qa_0(x)$ tend to the nonzero limits $a_{-1}(x)$ and $\varrho^{-1}a_{-1}(x)$, respectively, and the gauge field $a_0(x)$ therefore does not decouple from the kink-Q-ball system. Due to this, the limiting solutions $f_0(x)$ and $s_0(x)$ are different from the corresponding non-gauged solutions $f_{\mathrm{k}}(x)$ and $s_{\mathrm{q}}(x)$, respectively. From Eqs. (84b)–(84f) it follows that the components of the soliton energy $E^{(G)}$, $E^{(T)}$, $E^{(P)}$, the total soliton energy E, and the Noether charges Q_{χ} and Q_{ϕ} also tend to finite values as $e = \varrho q \to \infty$. Hence, the electric charges of the kink and Q-ball components increase indefinitely in this regime, despite the fact that the electric field energy $E^{(E)}$ tends to zero. This is only possible if electric charge density (32) tends to zero as $e = \varrho q \to \infty$. Based on this, we can obtain the limiting relation between the coefficient functions of asymptotic expansions (82) and (83):

$$a_{-1}(x) \to \frac{\varrho\omega s_0(x)^2}{\varrho^2 f_0(x)^2 + s_0(x)^2} \tag{85}$$

as the gauge coupling constants $e = \varrho q \to \infty$.

Let us discuss the behaviour of the asymptotic expansions in the two extreme regimes. In the regime $e = \varrho q \to 0$, the leading terms of asymptotic expansions (80)–(81) are linear in e. This is due to the linear dependence of $s(x)$ on e in Eq. (79b). In turn, this linear dependence results from the fact that differential equation (31) contains the term $-2q\omega a_0(x)s(x) \to -2\varrho^{-1}e\omega\alpha s(x)$, which is linear in e. From Eq. (31) it follows that $s(x)$ is invariant under the transformation $e \to -e$, $q \to -q$, $a_0 \to -a_0$, and thus coefficient function $s_1(x)$ changes sign under this transformation. Due to this, the coefficients $E^{(E)}_1$, $E^{(G)}_1$, $E^{(P)}_1$, $E^{(T)}_1$, and Q_1 also change sign under this transformation. Thus, the Noether charges, the components of the soliton energy, and the total soliton energy are invariant under the transformation $e \to -e$, $q \to -q$, $a_0 \to -a_0$ as expected. We can compare this situation with that of the opposite regime, $e = \varrho q \to \infty$. In this case, the asymptotic expansion of the electromagnetic potential $a_0(x)$ has the form (82), and so the term $-2q\omega a_0(x)s(x)$ in Eq. (31) transforms into the term $-2\varrho^{-1}\omega\left(a_{-1}(x) + e^{-2}a_{-3}(x)\right)s(x)$, which has no linear dependence on e. As a result, differential equations (30) and (31) contain only even inverse powers of e, and asymptotic expansions (83a) and (83b) therefore also contain only even inverse powers of e. Due to this, asymptotic expansions (84a)–(84f) also include only even inverse powers of e. The behaviour of the kink-Q-ball system in the extreme regimes $e = \varrho q \to 0$ and $e = \varrho q \to \infty$ was investigated using numerical methods, and was found to be in accordance with Eqs. (80), (81), (84), and (85).

Finally, we consider the plane-wave solution of gauge model (1). In this case, the gauge field A^{μ} and the scalar fields ϕ and χ are spread over the one-dimensional space and fluctuate around their vacuum values. Since the scalar field ϕ has the nonzero vacuum value $|\phi_{\mathrm{vac}}| = \eta$, the classical vacuum of model (1) is not invariant under local gauge transformations (6), meaning that the local gauge symmetry is spontaneously broken. For this reason, it is convenient to perform an investigation of the plane-wave solution in the unitary gauge $\mathrm{Im}(\phi(x,t)) = 0$. In this gauge, the Higgs mechanism is explicitly realized, and hence we can read off the particle composition of model (1). In the neighbourhood of the gauge vacuum $\phi_{\mathrm{vac}} = \eta$, $\chi_{\mathrm{vac}} = 0$, we have the complex scalar field χ with mass m_{χ}, the real scalar Higgs field ϕ_H with mass $m_{\phi} = \sqrt{2\lambda}\eta$, and the massive gauge field A^{μ} with mass $m_A = \sqrt{2}e\eta$.

We want to find the spatially uniform solution of field equations (9)–(11) that has the Noether charges Q_{ϕ} and Q_{χ} (recall that $eQ_{\phi} + qQ_{\chi} = 0$ for any finite energy field configuration) and to determine its energy. For this, we use field equations (9)–(11) in the unitary gauge. We assume that with unlimited spreading, the amplitudes of the complex scalar field χ and the real scalar Higgs field ϕ_H tend to zero, and that we can therefore neglect higher-order terms in the Lagrangian (1). For spatially uniform fields, the field equations for A^{μ} and ϕ_H become algebraic, whereas the field equation for χ determines the time dependence of χ. The solution was obtained for the case of a finite size L of the spatial dimension, and is presented as a series in inverse powers of L:

$$A^{\mu}_{\mathrm{pw}} = \left(\frac{q\lambda}{e^2 m^2_{\phi}}\frac{Q_{\chi}}{L} + O\left(\frac{1}{L^3}\right), 0\right), \tag{86}$$
$$\phi_{H\mathrm{pw}} = \frac{q^2}{e^2}\frac{\lambda^{3/2}}{\sqrt{2}m^5_{\phi}}\frac{Q^2_{\chi}}{L^2} + O\left(\frac{1}{L^4}\right), \tag{87}$$
$$\chi_{\mathrm{pw}} = \sqrt{\frac{Q_{\chi}}{2m_{\chi}L}}\left(1 + O\left(\frac{1}{L^4}\right)\right) \times \exp\left[-i\left(m_{\chi} + \frac{q^2}{e^2}\frac{\lambda}{m^2_{\phi}}\frac{Q_{\chi}}{L} + O\left(\frac{1}{L^3}\right)\right)t\right]. \tag{88}$$

As $L \to \infty$, the amplitudes of the fields A^0, ϕ_H, and χ tend to zero, whereas the phase frequency of the complex scalar field χ tends to m_χ. Note that the fields A^0, ϕ_H, and χ of the plane-wave solution tend to zero as L^{-1}, L^{-2}, and $L^{-1/2}$, respectively, and thus the Higgs field ϕ_H tends to zero much more quickly than the complex scalar field χ. Substituting Eqs. (86)–(88) into Eq. (8), we obtain the Noether charge densities j^0_ϕ and j^0_χ of the plane-wave solution:

$$j^0_\phi = -\frac{q}{e}\frac{Q_\chi}{L} + O\left(\frac{1}{L^5}\right), \tag{89}$$

$$j^0_\chi = \frac{Q_\chi}{L} + O\left(\frac{1}{L^5}\right). \tag{90}$$

From Eqs. (89) and (90) it follows that the electric charge of the plane-wave solution vanishes:

$$Q = \lim_{L\to\infty} L\left(e j^0_\phi + q j^0_\chi\right) = 0, \tag{91}$$

as expected. Next, we calculate the energies of the ϕ and χ components of the plane-wave solution:

$$E_\phi = \frac{q^2}{e^2}\frac{\lambda}{2m^2_\phi}\frac{Q^2_\chi}{L} + O\left(\frac{1}{L^3}\right), \tag{92}$$

and

$$E_\chi = m_\chi Q_\chi + O(L^{-4}), \tag{93}$$

giving a total energy of the plane-wave solution of

$$E_{\rm pw} = \lim_{L\to\infty}\left(E_\phi + E_\chi\right) = m_\chi Q_\chi. \tag{94}$$

We now discuss the results obtained here. Firstly, from Eqs. (92)–(94) it follows that the ϕ component does not contribute to the energy of the plane-wave solution as $L \to \infty$. At the same time, it follows from Eqs. (89) and (91) that the electric charge of the ϕ component does not vanish and is opposite to that of the χ component, meaning that the total electric charge of the plane-wave solution vanishes. Thus, the ϕ component contributes to the electric charge of the plane-wave solution, but does not contribute to its energy. This can be explained as follows. In the unitary gauge $\mathrm{Im}\,(\phi) = 0$, the real Higgs field ϕ_H fluctuates around the real vacuum average η, and the initial scalar field ϕ is written as $\phi = \eta + \phi_H$. Furthermore, from Eqs. (8a) and (14) we can obtain the electric charge and energy densities of the ϕ component of the plane-wave solution:

$$j^0_\phi = -2eA^0\left(\eta + \phi_H\right)^2 \sim -2e\eta^2 A^0 \tag{95}$$

and

$$\begin{aligned}\mathcal{E}_\phi &= \left(D_0\phi\right)^* D_0\phi + m^2_\phi \phi^2_H \\ &= e^2 A^2_0\left(\eta + \phi_H\right)^2 + m^2_\phi \phi^2_H \sim e^2\eta^2 A^2_0,\end{aligned} \tag{96}$$

where Eqs. (86) and (87) have been used. We see that in the leading order in L^{-1}, the Higgs field ϕ_H contributes neither to j^0_ϕ nor to $\mathcal{E}_\phi$, whereas the vacuum average of the scalar field ϕ contributes in both cases. We also see that as $L \to \infty$, the behaviour of j^0_ϕ and $\mathcal{E}_\phi$ is determined only by the electromagnetic potential A^0. At the same time, it follows from Eq. (86) that for the plane-wave solution, $A^0 \sim L^{-1}$, and thus $j^0_\phi \sim L^{-1}$ and $\mathcal{E}_\phi \sim L^{-2}$ in the leading order in L^{-1}. It follows that $Q_\phi = \int_{-\infty}^{+\infty} j^0_\phi dx = O\,(1)$ and $E_\phi = \int_{-\infty}^{+\infty} \mathcal{E}_\phi dx = O\left(L^{-1}\right)$, and therefore the ϕ component does not contribute to the energy of the plane-wave solution as $L \to \infty$.

5 Numerical results

To analyse the kink-Q-ball system, we must solve system of differential equations (29)–(31) subject to boundary conditions (34). This first boundary value problem can be solved only numerically. For this purpose, we use the boundary value problem solver provided in the MAPLE package [27]. To check the correctness of the numerical solutions, we use Eqs. (28), (36), and (53).

In order to solve the boundary value problem, we need to know eight dimensional parameters: $\omega, e, q, m_\phi = \sqrt{2\lambda}\eta, \lambda$, m_χ, g_χ, and h_χ. Without loss of generality, the mass m_χ can be chosen as the energy unit, and the dimensionless functions $a_0\,(x)$, $f\,(x)$, and $s\,(x)$ therefore depend only on the seven dimensionless parameters $\tilde{\omega} = \omega/m_\chi$, $\tilde{e} = e/m_\chi$, $\tilde{q} = q/m_\chi$, $\tilde{m}_\phi = m_\phi/m_\chi$, $\tilde{\lambda} = \lambda/m^2_\chi$, $\tilde{g}_\chi = g_\chi/m^2_\chi$, and $\tilde{h}_\chi = h_\chi/m^2_\chi$. In the present paper, we consider the kink-Q-ball system for which the dimensionless non-gauged parameters $\tilde{m}_\phi = \sqrt{2}$, $\tilde{\lambda} = 1$, $\tilde{g}_\chi = 2.3$, and $\tilde{h}_\chi = 1$ have the same order of magnitude. The dimensionless gauge coupling constants $\tilde{e}$ and $\tilde{q}$ are assumed to be equal to each other, and can take the values 0.05, 0.1, 0.15, 0.2, 0.3, 0.4, and 0.5.

We denote by ΔE the difference between the energies of the kink-Q-ball system and the non-gauged kink: $\Delta E = E - E_{\rm k}$, where $E_{\rm k} = 4\eta^3\sqrt{2\lambda}/3$. Figures 1 and 2 present the dependence of the dimensionless energy difference $\Delta\tilde{E} = \Delta E/m_\chi$ on the dimensionless phase frequency $\tilde{\omega}$. The curves in these figures correspond to the gauge coupling constants $\tilde{e} = \tilde{q}$, taking values from the set 0.1, 0.15, 0.2, 0.3, 0.4, and 0.5. Figure 1 presents the curves for the range between the minimum values of $\tilde{\omega}$, which we managed to reach by numerical methods, and the value $\tilde{\omega} = 0.88$. Figure 2 presents the same curves in the range from $\tilde{\omega} = 0.88$ to the maximum possible value $\tilde{\omega} = 1$. We use these two figures for a better representation of the dependences $\Delta\tilde{E}\,(\tilde{\omega})$.

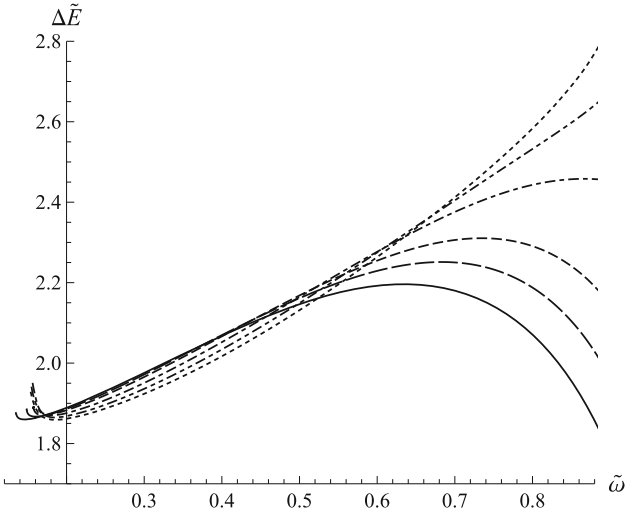

Fig. 1 Dependence of the dimensionless energy difference $\Delta\tilde{E}$ on the dimensionless phase frequency $\tilde{\omega}$. The solid, long-dashed, dashed, dash-dotted, dash-dot-dotted, and dotted curves correspond to the gauge coupling constants $\tilde{e} = \tilde{q} = 0.1$, 0.15, 0.2, 0.3, 0.4, and 0.5, respectively

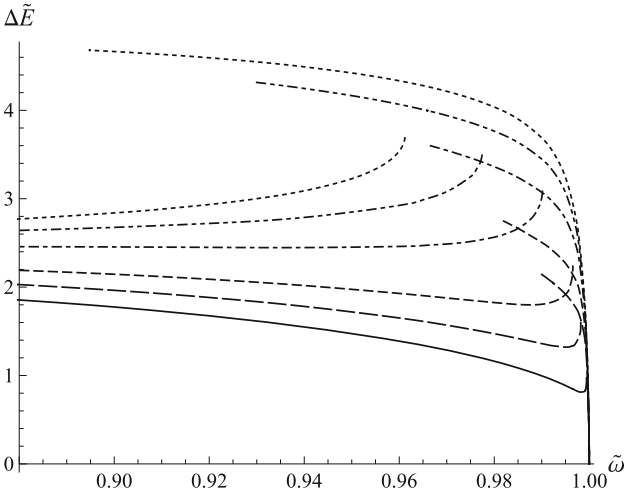

Fig. 2 Dependence of the dimensionless energy difference $\Delta\tilde{E}$ on the dimensionless phase frequency $\tilde{\omega}$. The notations of the curves are the same as in Fig. 1

For the same values of gauge coupling constants, the dependences $\Delta\tilde{E}\,(\tilde{\omega})$ and $Q_\chi\,(\tilde{\omega})$ are qualitatively similar, and the dependences $Q_\chi\,(\tilde{\omega})$ are therefore not given in the present paper.

Let us discuss the main features of the curves in Figs. 1 and 2. Firstly, we note that the energy of the kink-Q-ball system does not tend to infinity as $\tilde{\omega}$ tends to its minimum values (which depend on the gauge coupling constants). In fact, it was found numerically that the dependences $\tilde{E}\,(\tilde{\omega})$ and $Q_\chi\,(\tilde{\omega})$ have a branching point at $\tilde{\omega}_{\min}$:

$$\tilde{E} \sim A - B\tilde{\omega}_{\min}\,(\tilde{\omega} - \tilde{\omega}_{\min})^{1/2}\,, \tag{97}$$

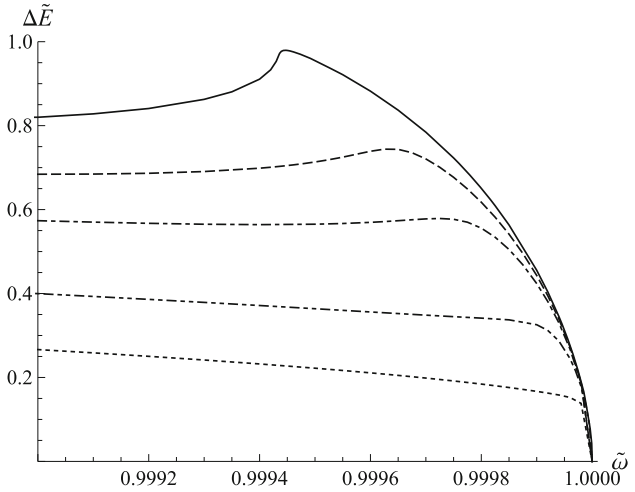

Fig. 3 Dependence of the dimensionless energy difference $\Delta\tilde{E}$ on the dimensionless phase frequency $\tilde{\omega}$ in the neighbourhood of $\tilde{\omega} = 1$. The dotted, dash-dot-dotted, dash-dotted, dashed, and solid curves correspond to the gauge coupling constants $\tilde{e} = \tilde{q} = 0.025$, 0.05, 0.075, 0.0875, and 0.1, respectively

$$Q_\chi \sim C - B\,(\tilde{\omega} - \tilde{\omega}_{\min})^{1/2}\,, \tag{98}$$

where A, B, and C are positive constants. We were unable to find any solutions to the boundary value problem for $\tilde{\omega} < \tilde{\omega}_{\min}$, and we therefore conclude that the kink-Q-ball system does not enter the thin-wall regime, in which both $\tilde{E}$ and Q_χ must tend to infinity. Note in this connection that a one-dimensional non-gauged Q-ball enters the thin-wall regime as the phase frequency $\tilde{\omega}$ tends to its minimal value [23]. In particular, in the case of self-interaction potential (4), the energy, the Noether charge, and the linear size of the one-dimensional Q-ball are proportional to $\ln\,(\tilde{\omega} - \tilde{\omega}_{\min})^{-1}$, meaning that they diverge logarithmically as $\tilde{\omega} \to \tilde{\omega}_{\min}$. However, this divergence is rather weak; for example, the energy and the Noether charge of a three-dimensional Q-ball with the same self-interaction potential are proportional to $(\tilde{\omega} - \tilde{\omega}_{\min})^{-3}$, whereas the size of the Q-ball is proportional to $(\tilde{\omega} - \tilde{\omega}_{\min})^{-1}$. At the same time, the electromagnetic interaction is strongest in one spatial dimension, as the Coulomb force does not depend on the distance between charges as long as the gauge symmetry is not broken. Thus we may suppose that the Coulomb interaction prevents the kink-Q-ball system from entering the thin-wall regime.

The behaviour of the curves in the neighbourhood of $\tilde{\omega} = 1$ is rather unusual. We see that for the gauge coupling constants $\tilde{e} = \tilde{q}$ from the set 0.15, 0.2, 0.3, 0.4, and 0.5, the dependence $\tilde{E}\,(\tilde{\omega})$ consists of two separate branches. The left branch starts from the minimal phase frequency $\tilde{\omega}_{\min}$ and continues until the maximum phase frequency $\tilde{\omega}_{\rm r}$. The behaviour of the left branch in the neighbourhood of $\tilde{\omega}_{\rm r}$ is similar to that in the neighbourhood of $\tilde{\omega}_{\min}$:

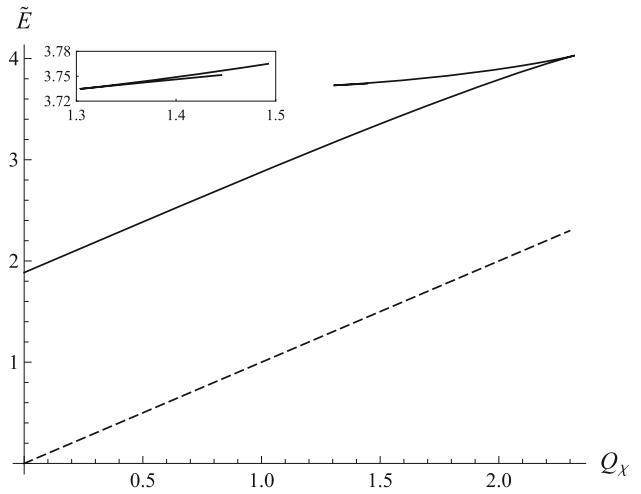

Fig. 4 Dependence of the dimensionless energy $\tilde{E}$ of the kink-Q-ball system with $\tilde{e} = \tilde{q} = 0.05$ on the Noether charge Q_χ (solid curve). The dashed line $\tilde{E} = Q_\chi$ corresponds to the plane-wave solution. The region in the neighbourhood of the upper left cusp point is shown on a larger scale

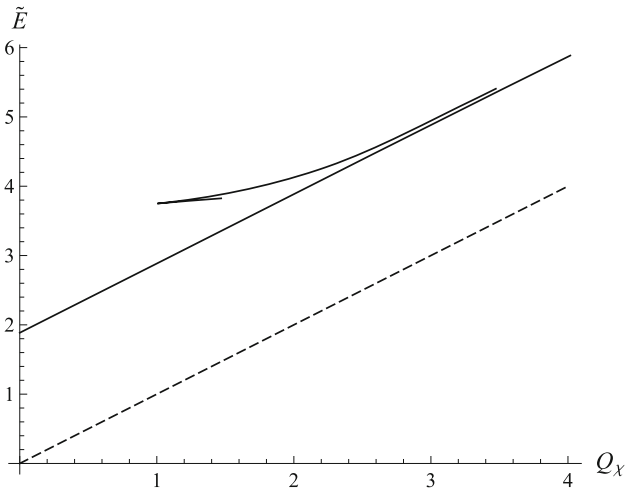

Fig. 5 Dependence of the dimensionless energy $\tilde{E}$ of the kink-Q-ball system with $\tilde{e} = \tilde{q} = 0.4$ on the Noether charge Q_χ (solid curve). The dashed line $\tilde{E} = Q_\chi$ corresponds to the plane-wave solution

$$\tilde{E} \sim D - F\tilde{\omega}_{\rm r}\left(\tilde{\omega}_{\rm r} - \tilde{\omega}\right)^{1/2}, \tag{99}$$

$$Q_\chi \sim G - F\left(\tilde{\omega}_{\rm r} - \tilde{\omega}\right)^{1/2}, \tag{100}$$

where D, F, and G are positive constants. The right branch starts from the point with the phase frequency $\tilde{\omega}_{\rm l} < \tilde{\omega}_{\rm r}$ and continues up to the maximum possible value of $\tilde{\omega}_{\rm tk} = 1$. The energy $\tilde{E}$ and the Noether charge Q_χ of the kink-Q-ball system reach maximum values at the starting point, as well as the electric charge $\tilde{q}Q_\chi$ of the Q-ball component. At the same time, the derivatives $d\tilde{E}/d\tilde{\omega}$ and $dQ_\chi/d\tilde{\omega}$ are finite at the starting point. Note that a similar situation also occurs for some three-dimensional gauged Q-balls [2,28]. The dependences $E(\omega)$ and $Q(\omega)$ of these Q-balls also reach maximum values at the limiting point of the phase frequency, while the derivatives $dE/d\omega$ and $dQ/d\omega$ are finite in this point. As $\tilde{\omega} \to 1$, the kink-Q-ball system enters the thick-wall regime. It was found numerically that in the neighbourhood of $\tilde{\omega}_{\rm tk} = 1$, $\Delta\tilde{E} \sim Q_\chi \sim H\left(\tilde{\omega}_{\rm tk} - \tilde{\omega}\right)^{1/2}$, in accordance with Eqs. (75) and (76).

Figure 3 shows the dependences $\Delta\tilde{E}(\tilde{\omega})$ for $\tilde{e} = \tilde{q} = 0.025$, 0.05, 0.075, 0.0875, and 0.1 in the neighbourhood of $\tilde{\omega}_{\rm tk} = 1$. Comparing Fig. 2 with Fig. 3, we see that with decreasing gauge coupling constants, the left and right branches are merged into one, and the dependence $\Delta\tilde{E}(\tilde{\omega})$ becomes single-valued. In accordance with Sect. 4, both curves in Fig. 3 enter the thick-wall regime as $\tilde{\omega} \to 1$.

Based on the dependences $\tilde{E}(\tilde{\omega})$ and $Q_\chi(\tilde{\omega})$, we can obtain the dependence $\tilde{E}\left(Q_\chi\right)$. Figures 4 and 5 show the dependence $\tilde{E}\left(Q_\chi\right)$ for the gauge coupling constants $\tilde{e} = \tilde{q} = 0.05$ and $\tilde{e} = \tilde{q} = 0.4$, respectively. The straight lines $\tilde{E} = Q_\chi$ in these figures correspond to the plane-wave solution. We see that for $\tilde{e} = \tilde{q} = 0.05$, the dependence $\tilde{E}\left(Q_\chi\right)$ is a single connected curve, whereas for $\tilde{e} = \tilde{q} = 0.4$, it consists of two separate curves. Of course, the number of curves in Figs. 4 and 5 is determined by the number of corresponding curves in Fig. 2. The curves in Figs. 4 and 5 possess cusps, the number of which is determined by the number of extremes of the corresponding curves in Figs. 1 and 2. The second derivative $d^2\tilde{E}/dQ_\chi^2$ changes sign when passing through the cusps or discontinuities, meaning that the convex and concave sections of the curves change each other. Note that in Figs. 4 and 5, the energy of the kink-Q-ball system turns out to be greater than the energy of the plane-wave solution with the same value of Q_χ. This also turns out to be true for all other cases considered in the present paper. It follows that the kink-Q-ball system may transit into the plane-wave field configuration through quantum tunnelling.

We now turn to the numerical kink-Q-ball solutions. It was found that the solutions that correspond to the left and right branches of the dependence $\tilde{E}(\tilde{\omega})$ are significantly different, so we consider the two solutions, one for each branch. Figure 6 shows the kink-Q-ball solution that corresponds to the dimensionless phase frequency $\tilde{\omega} = 0.985$ and belongs to the left branch. The energy density, the electric charge density, and the electric field strength corresponding to this kink-Q-ball solution are presented in Fig. 7. We see that in accordance with Sect. 3, $a_0(x)$ and $s(x)$ are even functions of x, whereas $f(x)$ is an odd function of x. From Fig. 7, it follows that the kink-Q-ball system possesses symmetrical energy and electric charge densities, and a nonzero electric field strength that is an odd function of the space coordinate. The distribution of the electric charge density is a centrally symmetric peak with a positive j_0 surrounded by two areas with a negative j_0, and thus the total electric charge of the kink-Q-ball system vanishes. The central positive peak is due to the contribution

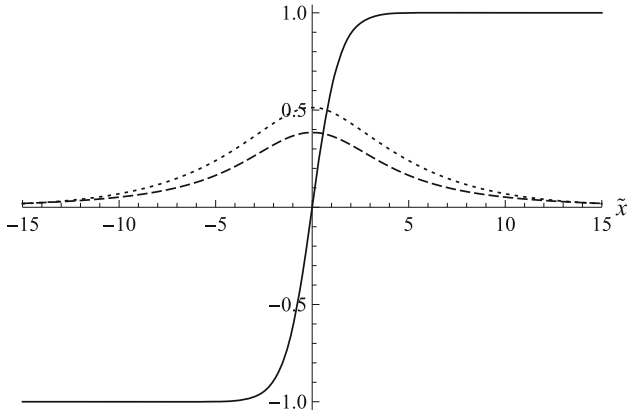

Fig. 6 The numerical kink-Q-ball solution from the left branch in Fig. 2 corresponding to $\tilde{e} = \tilde{q} = 0.2$ and $\tilde{\omega} = 0.985$. The solid, dashed, and dotted curves correspond to $f(\tilde{x})$, $s(\tilde{x})$, and $a_0(\tilde{x})$, respectively

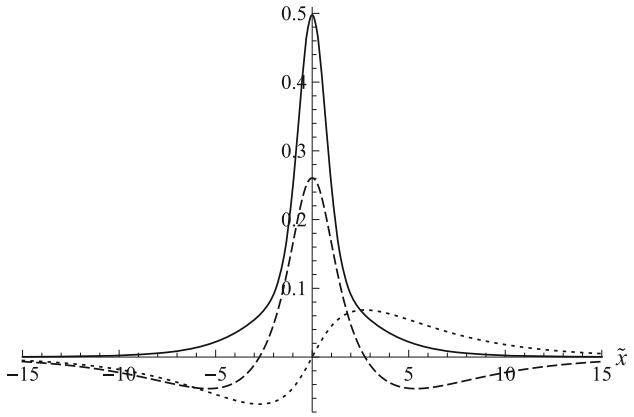

Fig. 7 Dimensionless versions of the scaled energy density $0.4\tilde{\mathcal{E}} = 0.4 m_\chi^{-2}\mathcal{E}$ (solid curve), the scaled electric charge density $\tilde{e}^{-1}\tilde{j}_0 = \tilde{e}^{-1} m_\chi^{-2} j_0$ (dashed curve), and the electric field strength $\tilde{E}_x = m_\chi^{-1} E_x$ (dotted curve) corresponding to the kink-Q-ball solution in Fig. 6

of the field χ, whereas the two negative areas to the sides are due to the contribution of the field ϕ. Indeed, from Eq. (32), it follows that the electric charge density of the field ϕ is $-2a_0 e^2 f^2$. We see that the electromagnetic potential a_0 can induce a nonzero electric charge density even if the scalar field ϕ approaches the vacuum value $|\eta|$. As a result, a substantial part of the electric charge of the complex scalar field ϕ comes from the two side regions where $|\phi| \approx |\eta|$.

In Fig. 8, we can see the kink-Q-ball solution that corresponds to the same phase frequency $\tilde{\omega} = 0.985$ as the previous one but belongs to the right branch in Fig. 2. The densities of the energy and the electric charge are presented in Fig. 9 along with the electric field strength. The solution presented in Fig. 8 differs drastically from the solution presented in Fig. 6. Unlike Fig. 6, the ansatz functions $s(\tilde{x})$ and $a_0(\tilde{x})$ have two widely separated symmetrical maxima. At the same time, the form of the kink component changed insignificantly in comparison with that in Fig. 6. Note that

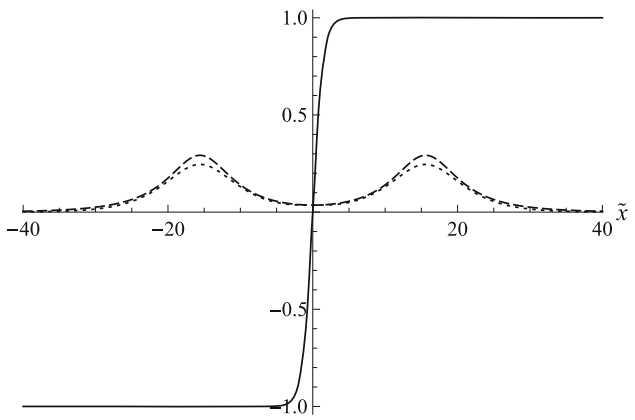

Fig. 8 The numerical kink-Q-ball solution from the right branch in Fig. 2 corresponding to $\tilde{e} = \tilde{q} = 0.2$ and $\tilde{\omega} = 0.985$. The solid, dashed, and dotted curves correspond to $f(\tilde{x})$, $s(\tilde{x})$, and $a_0(\tilde{x})$, respectively

in accordance with Eqs. (48) and (50), the electromagnetic potential $a_0(\tilde{x})$ also has a weak local maximum at $\tilde{x} = 0$, which is not discernible in Fig. 8. The densities $\mathcal{E}$ and j^0 in Fig. 9 also differ considerably from those in Fig. 7. Firstly, the energy density $\mathcal{E}$ has the sharp central peak and the two symmetrical side peaks. The central peak is due to the kink component, whereas the two side peaks result from the Q-ball component of the soliton solution. Secondly, the distribution of the electric charge density j_0 consists of two symmetrical side peaks with a positive j_0, each of which surrounded by two regions with a negative j_0. Note that in accordance with Eq. (50), there is also the local positive maximum of j_0 at $\tilde{x} = 0$.

The kink-Q-ball solutions presented in Figs. 6 and 8 belong to the different branches of $\tilde{E}(\tilde{\omega})$ but correspond to the same phase frequency. However, if we compare kink-Q-ball solutions corresponding to different phase frequencies, the situation does not undergo qualitative changes. Solutions from the left branch are similar to the solution in Fig. 6, whereas those from the right branch are similar to the solution in Fig. 8. For $\tilde{e} = \tilde{q} \lesssim 0.11$, the left and right branches are merged into a single curve $\tilde{E}(\tilde{\omega})$, as shown in Fig. 3. In this case, there exists a transition phase frequency $\tilde{\omega}_{\rm tr}$ (that depends on the gauge coupling constants) such that for $\tilde{\omega} \in (\tilde{\omega}_{\rm min}, \tilde{\omega}_{\rm tr})$, the solution is of the type shown in Fig. 6, whereas for $\tilde{\omega} \in (\tilde{\omega}_{\rm tr}, 1)$, the solution is of the type shown in Fig. 8. The transition between the two types of solutions is continuous and occurs at $\tilde{\omega} = \tilde{\omega}_{\rm tr}$.

Thus the Q-ball component of kink-Q-ball solutions is of the two-peak form when $\tilde{\omega}$ is in a close neighbourhood of unity. The further fate of the kink-Q-ball system is determined by the two factors: the self-interaction and the Coulomb repulsion of the complex scalar field χ. The self-interaction of the scalar field χ leads to the attraction between the two peaks. This is because the non-gauged Q-ball has the

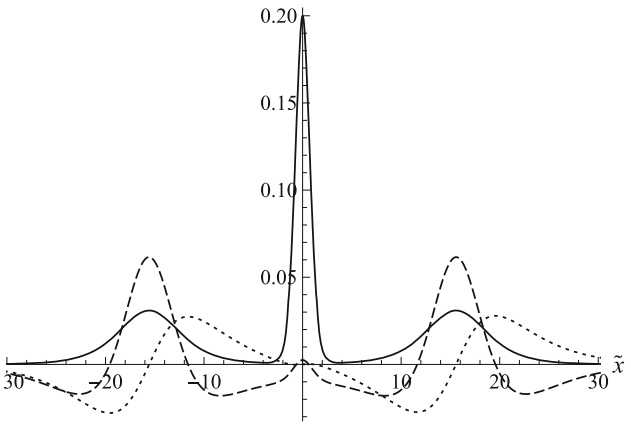

Fig. 9 Dimensionless versions of the scaled energy density $0.2\tilde{\mathcal{E}} = 0.2m_\chi^{-2}\mathcal{E}$ (solid curve), the scaled electric charge density $\tilde{e}^{-1}\tilde{j}_0 = \tilde{e}^{-1}m_\chi^{-2}j_0$ (dashed curve), and the electric field strength $\tilde{E}_x = m_\chi^{-1}E_x$ (dotted curve) corresponding to the kink-Q-ball solution in Fig. 8

one-peak form and possesses a minimum energy at the fixed Noether charge Q_χ. It follows that in the non-gauged case, the energy of the two-peak configuration is greater than the energy of the one-peak configuration at the fixed Q_χ, and thus the two-peak configuration will seek to the merging. On the other hand, the two peaks of the gauged Q-ball component will experience the Coulomb repulsion. Note that due to the breaking of the gauge symmetry, the Coulomb interaction is short-ranged. Moreover, there exists a partial neutralization of the electric charge densities of the kink and Q-ball components. However, the kink scalar field ϕ vanishes at $x = 0$, so the screening of the Coulomb interaction is considerably weakened in the neighbourhood of $x = 0$. Moreover, the electric charge density of the kink component also vanishes at $x = 0$, so the neutralization effect is also considerably weakened in this spatial region. The Coulomb repulsion between the two peaks increases with increasing the gauge coupling constant $\tilde{q}$. Thus if the gauge coupling constant is small, the attraction between the two peaks overpowers the Coulomb repulsion, and thus the two peaks merge into one at $\tilde{\omega} = \tilde{\omega}_{\text{tr}}$. In this case, the dependence $\tilde{E}(\tilde{\omega})$ is a single curve. If the gauge coupling constant $\tilde{q} \gtrsim 0.11$, the Coulomb repulsion overpowers the attraction between the two peaks, and thus the kink-Q-ball system remains in the two-peak form. In this case, the dependence $\tilde{E}(\tilde{\omega})$ splits into the left and right branches, which correspond to the one-peak and two-peak forms of the kink-Q-ball system, respectively. Due to Eq. (28), the dependence $Q_\chi(\tilde{\omega})$ is also a single curve as $\tilde{e} = \tilde{q} \lesssim 0.11$ and splits into the left and right branches as $\tilde{e} = \tilde{q} \gtrsim 0.11$.

We now discuss the issue of the stability of the kink-Q-ball system. As has already been pointed out, the energy of the kink-Q-ball system turns out to be greater than the energy of the plane-wave solution with the same Q_χ, for all cases considered in the present paper. It follows that the kink-Q-ball system is unstable against transit into a plane-wave configuration via quantum tunnelling. We still need to consider the classical stability of the kink-Q-ball system with respect to fluctuations in the fields ϕ, χ, and A_μ in the functional neighbourhood of the kink-Q-ball solution.

It is known that the gauge model described by the first line of the Lagrangian (1) has a kink solution [19,20]. In the adopted gauge $A_x = 0$, this kink solution is given by Eq. (5). The gauged kink has zero electric charge, and therefore has finite energy. However, unlike the kink of a self-interacting real scalar field [29,30], the gauged kink is not a topologically stable field configuration. Due to the topological structure of the vacuum of the Abelian Higgs model, the gauged kink is a sphaleron [19,20], the existence of which is due to the paths in the functional space that connect the topologically distinct vacua of the Abelian Higgs model [31]. The sphaleron lies between two topologically distinct neighbouring vacua and has only one unstable mode.

The gauged kink is a static solution modulo gauge transformations. However, in the case of the kink-Q-ball solution, we have a different situation. It can easily be shown that the kink-Q-ball solution will depend on time in any gauge, and thus is not a static solution. It follows that the point in the functional space corresponding to the kink-Q-ball solution will vary with time in any gauge. This fact does not allow the kink-Q-ball solution to be a sphaleron, so the issue of the unstable modes of the kink-Q-ball solution should be investigated separately.

To investigate the classical stability of the kink-Q-ball system, it is necessary to consider the second-order variation $\delta^2 E$ in the energy of system. Moreover, the fields of the model must fluctuate so that the Noether charges Q_ϕ and Q_χ remain fixed [21] and the perturbed electromagnetic potential satisfies Gauss's law. As a result, the second-order variation for fixed Q_ϕ and Q_χ is written as $\delta^2 E = \int\int_{-\infty}^{+\infty} \psi^T(x)\,\mathcal{K}\left(x, x'\right)\psi\left(x'\right)dxdx'$, where $\mathcal{K}$ is a linear symmetric integro-differential operator and $\psi = (\delta\phi_1, \delta\phi_2, \delta\chi_1, \delta\chi_2)$ is a fluctuation in the model's scalar fields $\phi = \phi_1 + i\phi_2$ and $\chi = \chi_1 + i\chi_2$. Note that the perturbation in the electromagnetic potential is not included in ψ, since it must be expressed in terms of the fluctuations in the scalar fields using Gauss's law. Thus to study the stability of the kink-Q-ball system, we must find the eigenvalues and eigenmodes of the complicated integro-differential operator: $\int_{-\infty}^{+\infty} \mathcal{K}\left(x, x'\right)\psi_i\left(x'\right)dx = \lambda_i\psi_i(x)$, where the eigenmodes ψ_i form a complete orthonormal set of real functions: $\int_{-\infty}^{+\infty} \psi_i^T\psi_j dx = \delta_{ij}$.

All of these factors make it difficult to study the spectrum of $\mathcal{K}$, even through the use of numerical methods. However, these difficulties can be avoided if we solve field equations (9)–(11) numerically, with a perturbed initial field configu-

ration in a close neighbourhood of the kink-Q-ball solution. To examine the stability of the kink-Q-ball system, we work in the temporal gauge $A_0 = 0$. In this gauge, the time evolution of the fields ϕ_1, ϕ_2, χ_1, χ_2, and A_x is determined by a system of five differential equations, each of which includes the second-order time derivative of one of the fields. This circumstance make it easier to study the time evolution of the perturbed kink-Q-ball system by numerical methods. At $t = 0$, the perturbed kink-Q-ball system must satisfy Gauss's law and must have the same Q_ϕ and Q_χ as the unperturbed kink-Q-ball system. The field equations then guarantee that for $t > 0$, Gauss's law is satisfied and the perturbed kink-Q-ball system possesses the same Q_ϕ and Q_χ as the unperturbed one. Having obtained the perturbed and unperturbed kink-Q-ball solutions, we can observe the behaviour of the field perturbations as time passes. If any field perturbation oscillates in a neighbourhood of the unperturbed kink-Q-ball solution, then the solution is classically stable. If at least one field perturbation exists that increases exponentially with time, then the kink-Q-ball solution is classically unstable.

In the present paper, we investigate the stability of the kink-Q-ball system for $\tilde{e} = \tilde{q} = 0.05$, 0.1, 0.15, 0.2, 0.3, 0.4, and 0.5. For all values of the gauge coupling constants, we take the step of changing of $\tilde{\omega}$ equal to 0.1. To solve field equations (9)–(11), we use the solver of partial differential equations provided in the MAPLE package [27]. We find that there are at least two initial field perturbations that lead to instability in the kink-Q-ball system. These unstable initial field perturbations are

$$\Psi_1 = \left(0, \alpha \operatorname{sech}\left(m_\phi x/2\right), 0, 0\right), \tag{101}$$

$$\Psi_2 = \left(0, 0, 0, \beta \operatorname{sech}\left(m_\chi x/2\right) \tanh(m_\chi x/2)\right), \tag{102}$$

where α and β are small constants. The constants α and β should be sufficiently small so that the initial perturbed field configuration lies in a close functional neighbourhood of the kink-Q-ball solution. We used values of α and β equal to 0.001 in our numerical calculations; however, whether or not a given perturbation is stable does not depend on specific values of α and β. It can be shown that at $t = 0$, the Noether charge densities j^0_χ and j^0_ϕ remain invariant under both perturbations (101) and (102), in the same way as the electric charge density $j^0 = e j^0_\phi + q j^0_\chi$.

The unstable perturbation Ψ_1 corresponds to the unstable eigenmode of the non-gauged complex kink [31], whereas the unstable perturbation Ψ_2 has no analogue in the non-gauged case since the one-dimensional non-gauged Q-ball corresponding to self-interaction potential (4) is stable [23]. The unstable perturbations Ψ_1 and Ψ_2 are orthogonal ($\int_{-\infty}^{+\infty} \Psi_1^T \Psi_2 dx = 0$) and have opposite parities. It follows that the perturbations Ψ_1 and Ψ_2 are expanded in terms of different eigenmodes of the operator $\mathcal{K}$, and thus the instabilities in Ψ_1 and Ψ_2 result from different unstable eigenmodes of $\mathcal{K}$. Thus the linear integro-differential operator $\mathcal{K}$ has at least two unstable eigenmodes. Note that the perturbations Ψ_1 and Ψ_2 are representatives of broader classes of unstable perturbations; that is, the initial field perturbations $\Xi_1 = (0, \delta\phi_2(x), 0, 0)$ and $\Xi_2 = (0, 0, 0, \delta\chi_2(x))$, where $\delta\phi_2(x)$ is an arbitrary even function and $\delta\chi_2(x)$ is an arbitrary odd function, are also unstable because their scalar products with the unstable perturbations Ψ_1 and Ψ_2 are different from zero: $\int_{-\infty}^{+\infty} \Xi_1^T \Psi_1 dx \neq 0$ and $\int_{-\infty}^{+\infty} \Xi_2^T \Psi_2 dx \neq 0$.

Using the graphical tools of the MAPLE package, we found that the unstable perturbations Ψ_1 and Ψ_2 increase exponentially with time and eventually destroy the kink-Q-ball system. We were able to estimate the exponential growth rate ν for the perturbations Ψ_1 and Ψ_2. For Ψ_1, the exponential growth rate $\nu \approx 0.6 \div 0.8$, whereas for Ψ_2, the exponential growth rate $\nu \approx 0.3 \div 0.5$, where the intervals in ν are due to the use of different gauge coupling constants and phase frequencies. We see that the exponential growth rates of Ψ_1 and Ψ_2 are different, so the time evolution of the perturbations Ψ_1 and Ψ_2 is determined by different unstable modes of the operator $\mathcal{K}$. Note that for the unstable eigenmode of the non-gauged kink, the exponential growth rate $\nu = m_\phi/2 \approx 0.707$. Thus, we can conclude that the time evolution of the perturbation Ψ_1 is determined by the unstable eigenmode of $\mathcal{K}$, which turns into the unstable eigenmode of the non-gauged complex kink as the gauge coupling constants vanish. The results obtained here show that the kink-Q-ball system is not a sphaleron since it has at least two unstable modes, whereas a sphaleron must have only one unstable mode.

6 Conclusion

In the present paper, we consider one-dimensional model (1), which consists of two self-interacting complex scalar fields interacting through an Abelian gauge field. It is shown that the model possesses a soliton solution consisting of a gauged kink and a gauged Q-ball. Since the finiteness of the energy of the one-dimensional soliton system leads to its electric neutrality, the gauged kink and the gauged Q-ball have opposite electric charges. Due to the neutrality of the Abelian gauge field, the opposite electric charges of the kink and Q-ball components are conserved separately, and despite the neutrality of the kink-Q-ball system, it possesses a nonzero electric field.

In the kink-Q-ball system, the energy and the Noether charge have rather unusual dependences on the phase frequency. It is shown here that the energy and the Noether charge of the kink-Q-ball system do not tend to infinity as the phase frequency tends to its minimum value. It follows that there is no thin-wall regime for the kink-Q-ball system. We also find that when the magnitude of the phase frequency is

in the neighbourhood of m_χ, the dependences of the energy and the Noether charge on the phase frequency consist of two separate branches, provided that the model's gauge coupling constants are large enough. The solutions from the left branches have a one-peak form, whereas those from the right branches have a two-peak form. In all cases, however, the kink-Q-ball system enters the thick-wall regime as the magnitude of the phase frequency tends to m_χ.

In addition to the kink-Q-ball solution, the model also possesses a plane-wave solution. For all sets of model parameters considered in the present paper, the energy of the kink-Q-ball solution turns out to be greater than the energy of the plane-wave solution for the same value of the Noether charge. Due to the topological structure of the vacuum of the model, the kink-Q-ball solution is not topologically stable, meaning that it can transit into the plane-wave configuration through quantum tunnelling.

It is well-known that the Abelian Higgs model possesses a gauge kink solution. The gauge kink is electrically neutral and has one unstable mode. From the viewpoint of topology, the gauge kink is a static (modulo gauge transformations) field configuration lying between two topologically distinct adjacent vacua. In contrast, the kink-Q-ball solution depends on time in any gauge, meaning that it is not a static field configuration. Hence, the kink-Q-ball solution cannot be a sphaleron, and its classical stability requires separate consideration. We investigate the classical stability of the kink-Q-ball system by means of a numerical solution of the field equations, with initial field configurations perturbed in a close neighbourhood of the kink-Q-ball solution. In all cases considered, it was found that the kink-Q-ball solution has at least two unstable modes, and thus it is even more unstable than the gauged kink.

Acknowledgements This work was supported by the Russian Science Foundation, Grant No. 19-11-00005.

Data Availability Statement This manuscript has no associated data or the data will not be deposited. [Authors' comment: This paper does not use any additional data.]

References

1. B. Julia, A. Zee, Phys. Rev. D **11**, 2227 (1975)
2. K. Lee, J.A. Stein-Schabes, R. Watkins, L.M. Widrow, Phys. Rev. D **39**, 1665 (1989)
3. K.N. Anagnostopoulos, M. Axenides, E.G. Floratos, N. Tetradis, Phys. Rev. D **64**, 125006 (2001)
4. H. Arodz, J. Lis, Phys. Rev. D **79**, 045002 (2009)
5. I.E. Gulamov, E.Ya. Nugaev, M.N. Smolyakov, Phys. Rev. D **89**, 085006 (2014)
6. J. Hong, Y. Kim, P.Y. Pac, Phys. Rev. Lett. **64**, 2230 (1990)
7. R. Jackiw, E.J. Weinberg, Phys. Rev. Lett. **64**, 2234 (1990)
8. R. Jackiw, K. Lee, E.J. Weinberg, Phys. Rev. D **42**, 3488 (1990)
9. D. Bazeia, G. Lozano, Phys. Rev. D **44**, 3348 (1991)
10. P.K. Ghosh, S.K. Ghosh, Phys. Lett. B **366**, 199 (1996)
11. S.K. Paul, A. Khare, Phys. Lett. B **174**, 420 (1986)
12. A. Khare, S. Rao, Phys. Lett. B **227**, 424 (1989)
13. A. Khare, Phys. Lett. B **255**, 393 (1991)
14. AYu. Loginov, V.V. Gauzshtein, Phys. Lett. B **784**, 112 (2018)
15. C. dos Santos, E. da Hora, Eur. Phys. J. C **70**, 1145 (2010)
16. L. Losano, J.M.C. Malbouisson, D. Rubiera-Garcia, C. dos Santos, EPL **101**, 31001 (2013)
17. AYu. Loginov, V.V. Gauzshtein, Phys. Rev. D **99**, 065011 (2019)
18. AYu. Loginov, Phys. Lett. B **777**, 340 (2018)
19. A.I. Bochkarev, M.E. Shaposhnikov, Mod. Phys. Lett. A **2**, 991 (1987)
20. DYu. Grigoriev, V.A. Rubakov, Nucl. Phys. B **299**, 67 (1988)
21. R. Friedberg, T.D. Lee, A. Sirlin, Phys. Rev. D **13**, 2739 (1976)
22. S. Coleman, Nucl. Phys. B **262**, 263 (1985)
23. T.D. Lee, Y. Pang, Phys. Rep. **221**, 251 (1992)
24. A. Kusenko, Phys. Lett. B **404**, 285 (1997)
25. T. Multamaki, I. Vilja, Nucl. Phys. B **574**, 130 (2000)
26. F. Paccetti Correia, M.G. Schmidt, Eur. Phys. J. C **21**, 181 (2001)
27. Maple User Manual (Maplesoft, Waterloo, Canada, 2019). https://www.maplesoft.com
28. Y. Brihaye, V. Diemer, B. Hartmann, Phys. Rev. D **89**, 084048 (2014)
29. R.F. Dashen, B. Hasslacher, A. Neveu, Phys. Rev. D **10**, 4130 (1974)
30. A.M. Polyakov, JETP Lett. **20**, 194 (1974)
31. N. Manton, P. Sutclffe, *Topological Solitons* (Cambridge University Press, Cambridge, 2004)